

Observational tests of the evolution of spheroidal galaxies

L. Silva¹, G. De Zotti^{2,4}, G. L. Granato^{2,4}, R. Maiolino³ & L. Danese⁴

¹INAF - Osservatorio astronomico di Trieste, Via Tiepolo 11, I-34131 Trieste, Italy

²INAF - Osservatorio astronomico di Padova, Vicolo dell'Osservatorio 5, I-35122 Padova, Italy

³INAF - Osservatorio astrofisico di Arcetri, Largo E. Fermi 5, I-50125 Firenze, Italy

⁴SISSA, Via Beirut 2, I-34014 Trieste, Italy

Accepted. Received

ABSTRACT

Granato et al. (2004a) have elaborated a physically grounded model exploiting the mutual feedback between star-forming spheroidal galaxies and the active nuclei growing in their cores to overcome, in the framework of the hierarchical clustering scenario for galaxy formation, one of the main challenges facing such scenario, i.e. the fact that massive spheroidal galaxies appear to have formed much earlier and faster than predicted by previous semi-analytical models, while the formation process was slower for less massive objects. After having assessed the values of the two parameters that control the effect of the complex and poorly understood radiative transfer processes on the time-dependent spectral energy distributions (SEDs), we have compared the model predictions with a variety of IR to mm data. Our results support a rather strict continuity between objects where stars formed (detected by (sub)-mm surveys) and evolved massive early-type galaxies, indicating that large spheroidal galaxies formed most of their stars when they were already assembled as single objects. The model is remarkably successful in reproducing the observed redshift distribution of $K \leq 20$ galaxies at $z > 1$, in contrast with both the classical monolithic models (which overestimate the density at high- z) and the semi-analytic models (that are systematically low), as well as the ratio of star-forming to passively evolving spheroids and the counts and redshift distributions of Extremely Red Objects (EROs), although the need of a more detailed modelling of the star formation history and of dust geometry is indicated by the data. The model also favourably compares with the ISOCAM 6.7 μ m counts, with the corresponding redshift distribution, and with Spitzer/IRAC counts, which probe primarily the passive evolution phase, and with the (sub)-mm SCUBA and MAMBO data, probing the active star-formation phase. The observed fraction of 24 μ m selected sources with no detectable emission in either the 8 μ m or R-band (Yan et al. 2004a) nicely corresponds to the predicted surface density of star-forming spheroids with 8 μ m fluxes below the detection limit. Finally, distinctive predictions for the redshift distributions of 24 μ m sources detected by Spitzer/MIPS surveys are pointed out.

Key words: galaxies: elliptical and lenticular, cD – galaxies: evolution – galaxies: formation – QSOs: formation

1 INTRODUCTION

The standard Lambda Cold Dark Matter (Λ CDM) cosmology is a well established framework to understand the hierarchical assembly of dark matter (DM) halos. Indeed, it has been remarkably successful in matching the observed large-scale structure. However the complex evolution of the baryonic matter within the potential wells determined by DM halos is still an open issue, both on theoretical and on observational grounds.

Full simulations of galaxy formation in a cosmological

setting are far beyond present day computational possibilities. Thus, it is necessary to introduce at some level rough parametric prescriptions to deal with the physics of baryons, based on sometimes debatable assumptions (e.g. Binney 2004). A class of such models, known as semi-analytic models, has been extensively compared with the available information on galaxy populations at various redshifts (e.g. Lacey et al. 1993; Kauffmann, White & Guiderdoni, 1993; Cole et al. 1994; Kauffmann et al. 1999; Somerville & Primack 1999; Cole et al. 2000; Granato et al. 2000; Benson et al. 2003; Baugh et al. 2004).

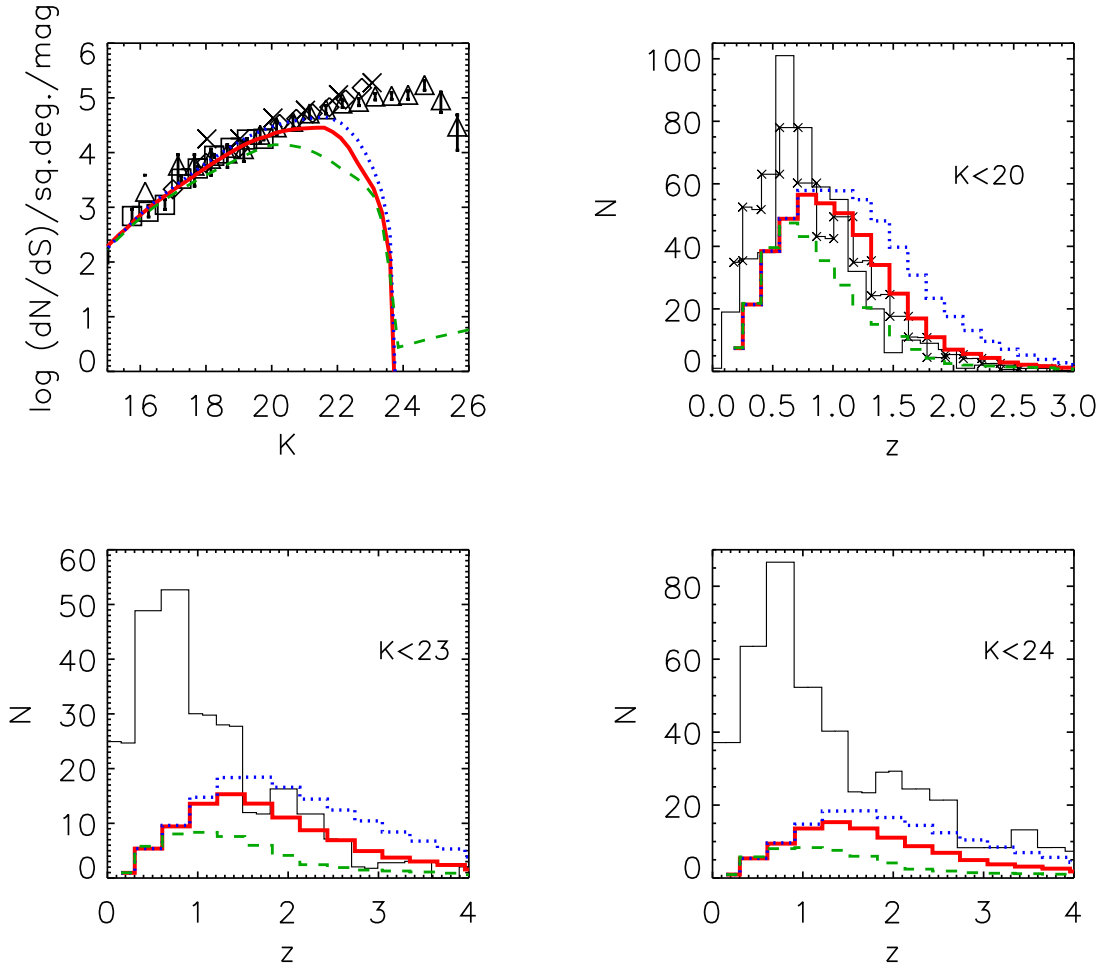


Figure 1. Contributions of spheroidal galaxies to the K -band number counts and redshift distributions of galaxies brighter than $K = 20$, 23, 24. The dashed, solid and dotted lines refer to $k = 3, 30, 300 M_{\odot}^{1/3}$ respectively (see Sect. 2.2). We adopt $k = 30 M_{\odot}^{1/3}$ as our reference value. Data for K band counts are from Moustakas et al. (1997), Kochanek et al. (2001), Saracco et al. (2001), Totani et al. (2001), Cimatti et al. (2002). In the upper-right panel (the $K < 20$ redshift distribution), the thin solid and the thin solid with crosses histograms (the redshift bin Δz is 0.15) are respectively from Cimatti et al. (2002) and Somerville et al. (2004) (scaled to the same area of the K20 survey). In the lower panels the thin continuous histograms ($\Delta z = 0.3$) are from Kashikawa et al. (2003).

The general strategy consists in using a subset of observations to calibrate the many model parameters providing a heuristic description of baryonic processes we don't properly understand. Besides encouraging successes, current semi-analytic models have met critical inconsistencies which seems to be deeply linked to the standard recipes and assumptions. These problems are in general related to the properties of elliptical galaxies, such as the color-magnitude and the $[\alpha/\mathrm{Fe}]$ -M relations (Cole et al. 2000; Thomas 1999; Thomas et al. 2002), and the statistics of sub-mm and deep IR selected (I- and K-band) samples (Silva 1999; Chapman et al. 2003; Kaviani et al. 2003; Daddi et al. 2004; Kashikawa et al. 2003; Poli et al. 2003; Pozzetti et al. 2003; Somerville et al. 2004). Discrepancies between the observationally estimated merger rate evolution and that predicted by semi-analytic models have also been reported (Conselice et al. 2003).

However, the general agreement of a broad variety of observational data with the hierarchical scenario and the fact

that the observed number of luminous high-redshift galaxies, while substantially higher than predicted by standard semi-analytic models, is nevertheless consistent with the number of sufficiently massive dark matter halos, indicates that we may not need alternative scenarios, but just some new ingredients or assumptions (see e.g. Baugh et al. 2004; Tecza et al. 2004).

Previous work by our group (Granato et al. 2001; Romano et al. 2002; Granato et al. 2004a) suggests that a crucial ingredient is the mutual feedback between spheroidal galaxies and active nuclei at their centers. Granato et al. (2004a, henceforth GDS04) presented a detailed physically motivated model for the early co-evolution of the two components, in the framework of the Λ CDM cosmology.

In this paper, we present a comparison of the model with the observed number counts and redshift distributions in several near-IR (NIR) to (sub)-mm bands.

In Section 2 we give a short overview of the GDS04 model for spheroidal galaxies, and we discuss the determina-

tion of the parameters controlling the time-dependent spectral energy distributions (SEDs) of spheroidal galaxies. In Section 3, the model predictions are compared with a variety of recent data. The main conclusions are summarized and discussed in Section 4.

We adopt the “concordance” cosmological model, with $\Omega_m = 0.3$, $\Omega_\Lambda = 0.7$, $H_0 = 70 \text{ km s}^{-1} \text{ Mpc}^{-1}$.

2 MODEL DESCRIPTION AND ASSESSMENT OF THE PARAMETERS

2.1 The GDS04 model

While referring to GDS04 for a full account of the model assumptions and their physical justification, we provide here, for the reader’s convenience, a brief summary of its main features.

The model follows with simple, physically grounded recipes and a semi-analytic technique the evolution of the baryonic component of proto-spheroidal galaxies within massive dark matter (DM) halos forming at the rate predicted by the standard hierarchical clustering scenario within a Λ CDM cosmology. The main novelty with respect to other semi-analytic models is the central role attributed to the mutual feedback between star formation and growth of a super massive black hole (SMBH) in the galaxy center. Further relevant differences are the assumption that the large scale angular momentum does not effectively slow down the collapse of the gas and the star formation in massive halos virialized at high redshift, and the allowance for a clumping factor, $C \simeq 20$, speeding up the radiative cooling so that even in very massive halos ($M_{\text{vir}} \sim 10^{13} M_\odot$), the gas, heated to the virial temperature, can cool on a relatively short (~ 0.5 –1 Gyr) timescale, at least in the dense central regions.

The GDS04 prescriptions are assumed to apply to DM halos virializing at $z_{\text{vir}} \gtrsim 1.5$ and $M_{\text{vir}} \gtrsim 4 \times 10^{11} M_\odot$. These cuts are meant to crudely single out galactic halos associated with spheroidal galaxies. Disk (and irregular) galaxies are envisaged as associated primarily to halos virializing at $z_{\text{vir}} \lesssim 1.5$, some of which have incorporated most halos less massive than $4 \times 10^{11} M_\odot$ virializing at earlier times, that may become the bulges of late type galaxies. However, the model does not address the formation of disk (and irregular) galaxies and these objects will not be considered in this paper. On the other hand, we do not expect that protospheroidal galaxies in the star-forming phase have already a spheroidal shape; rather they are likely to have an irregular, complex, disturbed morphology.

The kinetic energy fed by supernovae is increasingly effective, with decreasing halo mass, in slowing down (and eventually halting) both the star formation and the gas accretion onto the central black hole. On the contrary, star formation and black hole growth proceed very effectively in the more massive halos, giving rise to the bright SCUBA phase, until the energy injected by the active nucleus in the surrounding interstellar gas unbinds it, thus halting both the star formation and the black hole growth (and establishing the observed relationship between black hole mass and stellar velocity dispersion or halo mass). Not only the black hole growth is faster in more massive halos, but also the

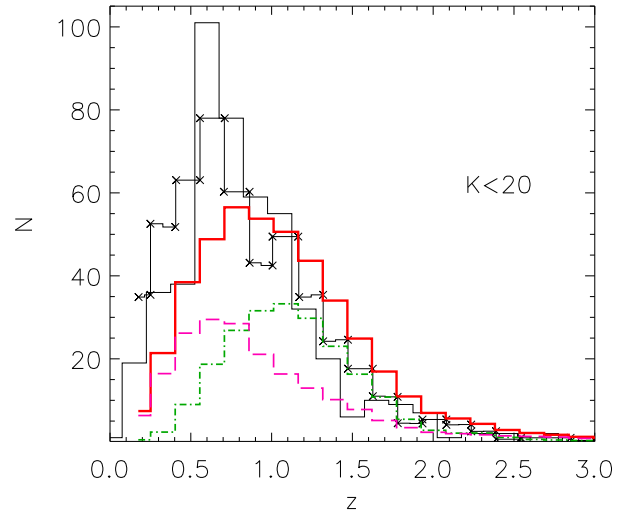


Figure 2. Contribution of star forming (dot-dashed line) and passively evolving (long-dashed line) spheroids to the $K < 20$ redshift distribution (the same as in Fig. 1). The thick solid line is the model total, the thin line the Cimatti et al. (2002) data, and the thin line with crosses the data from Somerville et al. (2004) scaled to the same area. Note that Somerville et al. give magnitudes in the AB system ($K_{AB} = K + 1.85$).

feedback of the active nucleus on the interstellar medium is stronger, to the effect of sweeping out such medium earlier, thus causing a shorter duration of the active star-formation phase. As a result, in keeping with the previous proposition by Granato et al. (2001), the physical processes acting on baryons reverse the order of formation of spheroidal galaxies with respect to the hierarchical assembling of DM halos, leading to the *Anti-hierarchical Baryon Collapse* (ABC) scenario.

2.2 Spectral energy distribution of spheroidal galaxies

As in GDS04, we compute the SEDs of spheroidal galaxies using our code GRASIL, described in Silva et al. (1998)¹. GRASIL computes the time-dependent UV to radio SED of galaxies, given their star formation and chemical enrichment histories (derived as described in GDS04), and with a state of the art treatment of dust reprocessing. The latter point is fundamental, since during the phase of intense star-formation, young stars are mixed with a huge amount of gas, quickly chemically enriched and dust polluted. The use of local templates (such as M82 or Arp220) may be inappropriate in these extreme conditions.

One of the most important distinctive features of GRASIL is that it has included, for the first time, the effect of *differential extinction* of stellar populations (younger stellar generations are more affected by dust obscuration), due

¹ The code is available at <http://adlibitum.oat.ts.astro.it/silva/default.html> or at <http://web.pd.astro.it/granato>

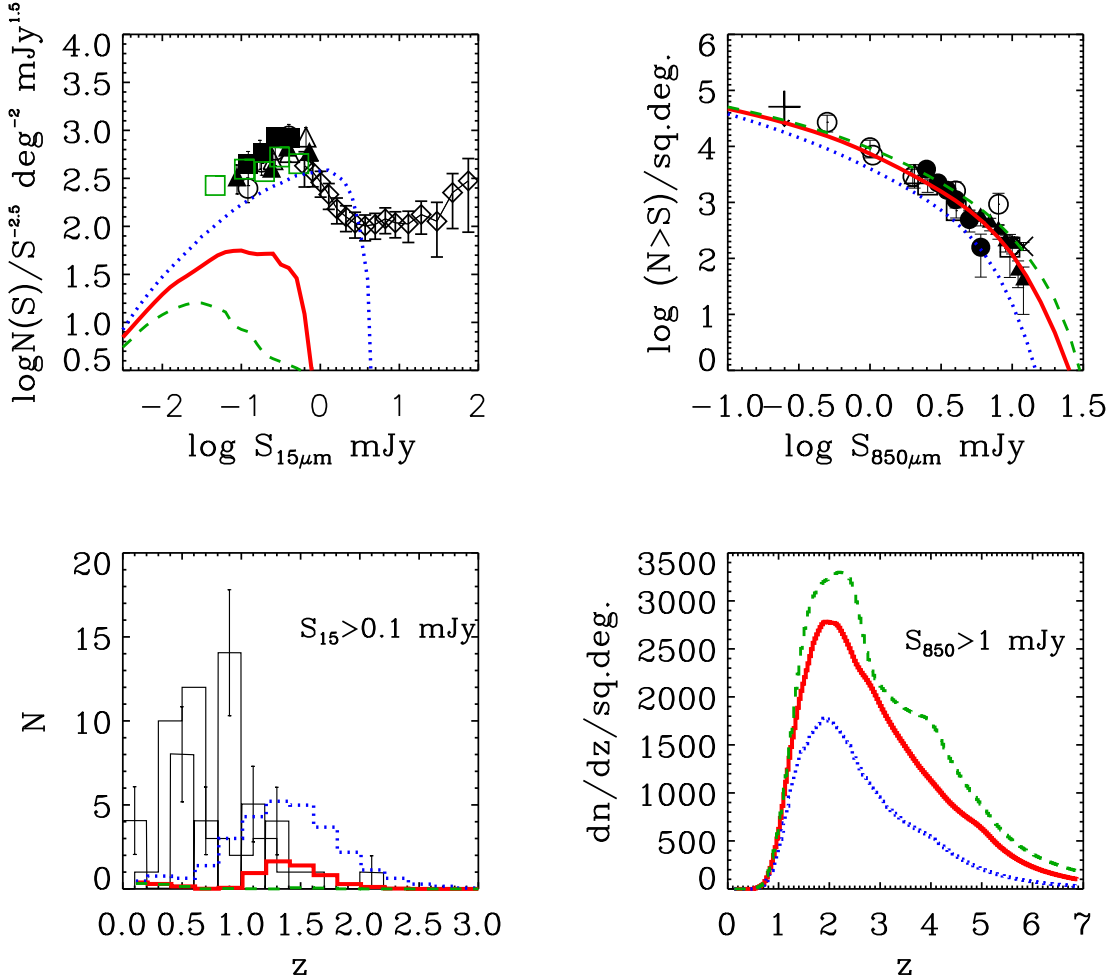


Figure 3. Possible contributions of spheroids to the observed 15 and 850 μm number counts and redshift distributions ($S_{15\mu\text{m}} > 0.1\text{mJy}$ within $6 \times 10^{-3} \text{ deg}^2$ and $\Delta z = 0.2$; $S_{850\mu\text{m}} > 1\text{mJy}$). The dotted, solid and dashed lines refer to $\tau_{\text{MC}}(1\mu\text{m}) \simeq 10, 60, 120$ respectively. The 15 μm data are from Elbaz et al. (1999), Gruppioni et al. (2002), Elbaz et al. (2002, thin histogram with error bars), Franceschini et al. (2003, thin histogram), Metcalfe et al. (2003). The 850 μm data are from Hughes et al. (1998), Barger, Cowie, & Sanders (1999), Blain et al. (1999), Eales et al. (2000), Borys et al. (2002), Chapman et al. (2002). A low $\tau_{\text{MC}}(1\mu\text{m})$ implies an excessive contribution from spheroids to the 15 μm counts, which are dominated by late-type, mainly starburst, galaxies at $z \lesssim 1$ (Hammer et al. 2004). On the other hand, a very high $\tau_{\text{MC}}(1\mu\text{m})$ overpredicts the 850 μm counts. Our reference model has $\tau_{\text{MC}}(1\mu\text{m}) = 60$. See text for details.

to the fact that stars form in a denser than average environment, the molecular clouds (MCs), and progressively get rid of them.

Radiative transfer results depend on the poorly known geometry of the system. Broadly speaking, predictions of fluxes during the active star forming phase become more and more affected by the ensuing model uncertainties at shorter and shorter wavelengths. In GDS04 we presented predictions for the dust-enshrouded SCUBA galaxies, or for the essentially dust-free passively evolving galaxies; in both cases, the results were insensitive to the details of the dust distribution. On the other hand, key information on the early evolution of spheroidal galaxies is provided by near-IR (particularly K -band) and mid-IR (ISO and Spitzer) data. To test the model against them we need a more careful investigation of the dependence of our results on the structure of galaxies.

In general, the GRASIL SEDs for spheroidal systems

depend on five structural parameters: the fraction f_{MC} of gas in the form of MCs rather than in the diffuse ISM (cirrus), the optical depth of MCs for a source at their center τ_{MC} (conventionally given at 1 μm hereafter), the escape timescale of newly born stars from MCs, t_e , and the core radii of the distributions of diffuse dust, r_c^c , and of stars outside MCs, r_c^* , assumed to follow a King (1972) law. In the following we will take $r_c^c = r_c^*$, and we will drop the superscript.

However, in the conditions envisaged here and for the purposes of the present work, the results are significantly affected only by τ_{MC} . This is proportional to the dust to gas mass ratio δ and to $M_{\text{MC}}/R_{\text{MC}}^2$, M_{MC} and R_{MC} being the typical mass and radius of molecular clouds, respectively. As for δ , we have simply assumed that it increases linearly with the gas metallicity (e.g., Dwek 1998) and is $\simeq 1/100$ (the Galactic value) for solar metallicity. Since the chemical evo-

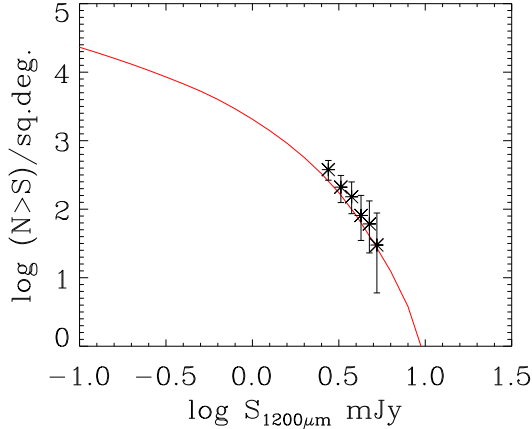


Figure 4. Integral counts of star-forming spheroidal galaxies at $1200\mu\text{m}$ predicted by our reference model, compared with MAMBO data from Greve et al. (2004).

lution of the galaxy is computed self-consistently, the true parameter is $M_{\text{MC}}/R_{\text{MC}}^2$, but we prefer to make reference to the value of τ_{MC} for solar metallicity (and thus $\delta \simeq 1/100$). We have checked that all the results presented here, except those on Extremely Red Objects (EROs, see Sect. 3.2), are very little affected by variations, within rather wide ranges, of the other GRASIL parameters.

However, an additional parameter is required to circumvent the problem that, for stars already outside their parent molecular clouds, GRASIL takes into account only the relatively small optical depth due to cirrus, neglecting that due to other MCs present along the line of sight. This is not necessarily accurate in the extreme conditions occurring during the fast star forming phase of spheroids, particularly in the dense central regions. In general, the mean optical depth to a star outside its parent MC is $\tau_{\text{outside}} = \tau_{\text{cirrus}} + (4/3)\bar{N}\tau_{\text{MC}}$, where we have assumed a uniform dust distribution inside MCs, and \bar{N} is mean number of MCs along its line of sight.

$$\bar{N} = S_f \frac{M_{\text{gas,MC}}}{M_{\text{MC}}} \frac{R_{\text{MC}}^2}{r_c^2} \propto M_{\text{gas,MC}} M_{\text{vir}}^{-2/3}, \quad (1)$$

where S_f is a shape factor and we have assumed $r_c \propto M_{\text{vir}}^{1/3}$, M_{vir} being the virial mass of the galaxy. Whenever $\bar{N} \ll 1$, the optical depth drops from τ_{MC} to τ_{cirrus} ($\ll 1$ at IR wavelengths) when the stars move out of their parent MCs. This condition is usually met in nearby galaxies. On the contrary, in forming spheroids τ_{outside} can be substantially larger than τ_{cirrus} . The shape factor S_f depends on the relative distribution of stars and MCs, and its value is also a function of the age of the stellar population under consideration: younger stars (but old enough to be out of molecular clouds) are on average closer to regions rich in MCs.

Thus, an accurate calculation of \bar{N} is extremely difficult, and we are forced to parameterize our ignorance. Also, the present release of GRASIL does not allow us to deal with the radiation transfer through the distribution of MCs. On the other hand, such detailed treatment is not crucial for our present purposes since whenever $\tau_{\text{outside}} \geq \tau_{\text{MC}}$ essentially all the starlight is reprocessed by dust. We have crudely approximated τ_{outside} as a step function: $\tau_{\text{outside}} = \tau_{\text{cirrus}}$ for

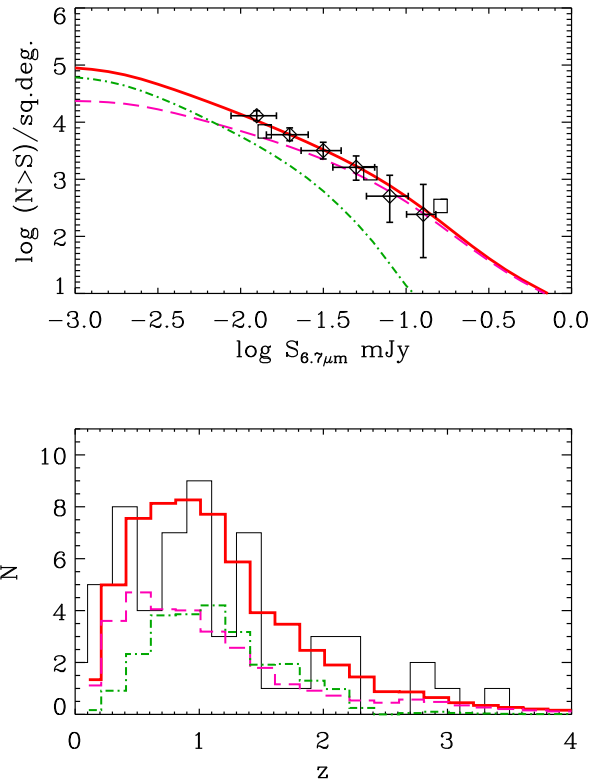


Figure 5. $6.7\mu\text{m}$ counts and redshift distribution of sources with $S_{6.7} > 10\mu\text{Jy}$ within 16 arcmin 2 . The thick solid line shows the prediction of our reference model (i.e. $k = 30 M_{\odot}^{1/3}$). The contributions of active and passive spheroids are represented by the dot-dashed and long-dashed lines respectively. The thin histogram in the lower panel shows the redshift distribution (with $\Delta z = 0.2$) observationally estimated by Sato et al. (2004). The observed counts are from Metcalfe et al. (2003, squares) and Sato et al. (2003, diamonds).

$M_{\text{gas,MC}} \leq k M_{\text{vir}}^{2/3}$ and $\tau_{\text{outside}} = \tau_{\text{cirrus}} + \tau_{\text{MC}}$ otherwise, treating k as an adjustable parameter. In order to take into account the dust heating by the absorbed starlight, in practice we have kept the stars within their MCs for the full duration of the starburst, for galaxies where $M_{\text{gas,MC}} > k M_{\text{vir}}^{2/3}$.

The parameter k affects mostly the results at $\lambda \lesssim 10\mu\text{m}$. The K -band counts and redshift distributions are best reproduced setting $k \sim 30 M_{\odot}^{1/3}$ (Fig. 1). Note that spheroids dominate the redshift distributions at substantial redshifts, while leaving room for other populations at low redshifts. The figure shows also the effect of varying k . In particular, a low value of k ($k \simeq 10$, not shown), would produce an almost perfect match of the $K < 20$ redshift distribution for $z \gtrsim 1$, but the contributions at $K < 23$ and $K < 24$ would decrease. A more detailed treatment of the complex behavior of the optical depth to stars outside MCs could improve the overall match, and will be considered for future releases of GRASIL.

The results in Fig. 1 refer to $t_e = 0.01$ Gyr, $f_{\text{MC}} = 0.5$ and $r_c = 0.1(M_{\text{vir}}/10^{12} M_{\odot})^{1/3}$ kpc, but change only marginally if t_e and f_{MC} vary within rather broad inter-

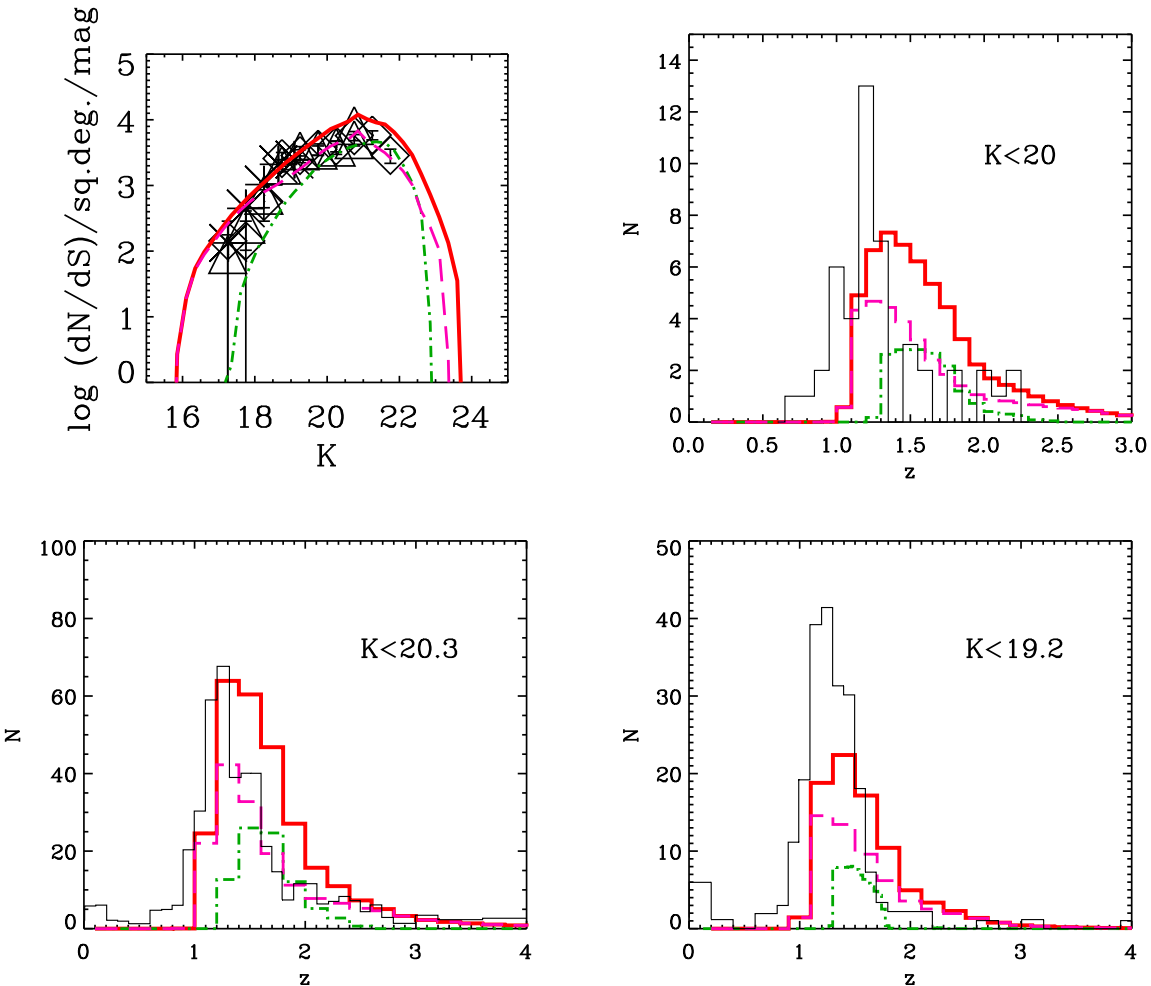


Figure 6. K -band counts and redshift distributions for EROs ($R - K > 5$). The thick solid line is the total predicted by our model, while the contributions of active and passive objects are shown by dot-dashed and long dashed lines respectively. Data from Daddi et al. (2000), Miyazaki et al. (2003), Roche et al. (2002, 2003), Cimatti et al. (2003). The redshift histograms are for $\Delta z = 0.1$ for $K < 20$, and for $\Delta z = 0.2$ in the two lower panels.

vals ($5 \text{ Myr} \lesssim t_e \lesssim 0.5 \text{ Gyr}$, $0.2 \lesssim f_{\text{MC}} \lesssim 0.9$), and r_c is increased or decreased by a factor of a few.

As for τ_{MC} , Silva et al. (1998) found that the SEDs of starburst galaxies are well reproduced by GRASIL with $\tau_{\text{MC}} \sim$ a few tens (a figure in reasonable agreement with direct observations of Giant Molecular Clouds in the Galaxy, for which $M_{\text{MC}} \sim 10^6 M_\odot$, $r_{\text{MC}} \sim 15 \text{ pc}$). However, the physical conditions in high- z star forming spheroids may be very different from those encountered in local systems, including starbursts and Ultra-Luminous IR Galaxies (ULIRGs). Thus, we have explored the generous range $3 < \tau_{\text{MC}} < 200$. This parameter controls the contribution (if any) of star-forming spheroidal galaxies to the bump in the $15 \mu\text{m}$ ISO-CAM counts below a few mJy. Although the observed counts are affected by a considerable uncertainty, as shown by the spread of results from different surveys, and the modelling is complicated by the presence of PAH bands, they have been interpreted by phenomenological models in terms of evolving starbursts, with a minor contribution from spirals, particularly at the brighter flux density levels (e.g. Franceschini et al. 2001; Gruppioni et al. 2002; Lagache et al. 2003;

Hammer et al. 2004). Thus, the contribution from star-forming spheroids must be substantially suppressed, implying $\tau_{\text{MC}} \gtrsim 40$ at $1 \mu\text{m}$ (see Fig. 3). A low value of τ_{MC} , and, correspondingly, a large contribution from spheroids to the sub-mJy bump of the $15 \mu\text{m}$ counts (upper-left panel), would entail a high- z tail of the redshift distribution of sources with $S_{15} > 0.1 \text{ mJy}$ substantially larger than indicated by current data (lower left-hand panel).

On the other hand, as illustrated by the right-hand panels of Fig. 3, an exceedingly large value of τ_{MC} would overproduce the $850 \mu\text{m}$ counts, while a very small value would underproduce them. The ensuing lower limit to τ_{MC} is however model dependent, since the effect of decreasing it may be compensated by a smaller value of the dust emissivity index, that we take equal to 2.

In the following we set $\tau_{\text{MC}} \simeq 60$ at $1 \mu\text{m}$, a value yielding $850 \mu\text{m}$ counts and redshift distributions consistent with the data, and a small, but non-negligible, contribution to the sub-mJy $15 \mu\text{m}$ counts.

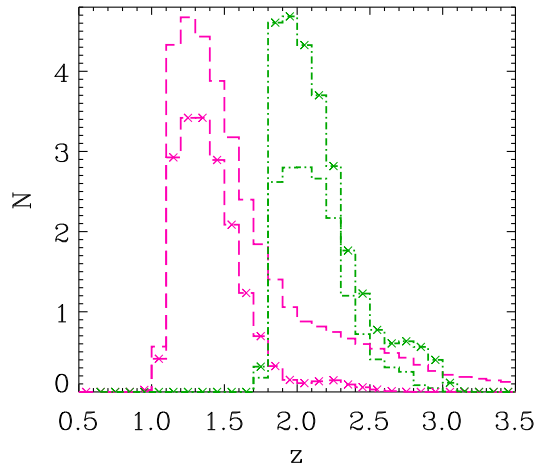


Figure 7. Dependence of predicted redshift distribution of EROs in the K20 survey on details of the model (see Fig. 6, upper right panel). The dashed line with crosses is obtained adding to the reference model (dashed line without crosses) a mild SF activity after the QSO phase (i.e. at the beginning of the passive evolution phase), at a level of 2% of the peak value and lasting 1 Gyr. The dot-dashed lines (for clarity these have been shifted by 0.5 in redshift) refer to objects before the QSO phase (i.e. in the active star-forming phase), adopting $t_e = 10$ Myr (line without crosses), or $t_e = 50$ Myr (with crosses).

3 COMPARISON WITH THE DATA

3.1 Counts and redshift distributions

As discussed by Granato et al. (2001, 2004a), in the present framework the SCUBA-selected galaxies are interpreted as being mostly star-forming massive proto-spheroidal galaxies ($M_{\text{vir}} \geq 10^{11.6} M_{\odot}$). The values of the GRASIL parameters derived above nicely fit the $850\mu\text{m}$ SCUBA counts (see Fig. 3, right-hand panels), and the latest MAMBO $1200\mu\text{m}$ data (Fig. 4). The model $850\mu\text{m}$ counts are almost undistinguishable from those already reported in Fig. 12 of GDS04, corresponding to a somewhat different choice of the parameters, and the redshift distributions are also essentially unchanged. Indeed, the predictions in the sub-mm region are not very sensitive to the precise values of GRASIL parameters, as far as proto-spheroidal galaxies are optically thick in the optical-UV. The predicted redshift distribution of sources brighter than 1mJy at $850\mu\text{m}$ has a broad peak at $z \sim 2$ with an extended tail towards higher redshifts, due to star-forming spheroidal galaxies. As already remarked in GDS04, this redshift distribution is in good agreement with the limited information available so far. In particular, the median redshift of the Chapman et al. (2003) sample ($S_{850\mu\text{m}} \geq 5\text{mJy}$) is 2.4, with a quartile range of $z = 1.9 - 2.8$. The median and quartile range for our model are 2.3 and 1.8 – 3.0.

While the sub-mm counts are informative on the star-formation phase of the evolution of spheroidal galaxies, the K -band counts (Fig. 1) in the range $14 \leq K \leq 17$ are dominated by the passive evolution phase. Fainter than $K \sim 17$ also star-forming spheroids begin to show-up and become increasingly important at fainter magnitudes. The brighter (in

terms of apparent magnitude) such objects are those of mass lower than the typical mass probed by present day sub-mm observations, i.e. those having, in the GDS04 model, a prolonged star-formation phase extending to $z \sim 1$, and whose stars have negligible obscuration as soon as they come out of their parent MC (see Sect. 2.2). This is illustrated by Fig. 2, showing that, for $K \leq 20$, the contribution from star-forming spheroids peaks at $z \sim 1$. In particular, the predicted number of spheroids with ongoing star formation at $1.4 < z < 2$ and $K < 20$ is about twice that of passive spheroids, and their typical stellar mass is between $5 \times 10^{10} M_{\odot}$ and $3 \times 10^{11} M_{\odot}$, in nice agreement with the findings of Daddi et al. (2004; see their Figure 5) and Somerville et al. (2004). The Star Formation Rate (SFR) of these active objects is $\lesssim 100 M_{\odot}\text{yr}^{-1}$: according to our model, the K band selects spheroids when their SF (and dust obscuration) is declining or after it has stopped. Daddi et al. (2004) measured a dust-corrected average SFR of $\simeq 200 M_{\odot}\text{yr}^{-1}$, higher than our expectations, but still well below the peak SFR of spheroids according to our scenario. This may suggest that the present version of our model envisages a too drastic decline of SF activity in intermediate mass objects (see also Sect. 3.2). Note also that Daddi et al. adopt a Salpeter IMF ($\propto M^{-1.35}$), while in the GDS04 model we have used a different IMF ($\propto M^{-1.25}$ above $1 M_{\odot}$, $\propto M^{-0.4}$ below) suggested by chemical constraints (see also Romano et al. 2002). This IMF implies a higher L/M ratio and, correspondingly, a SFR lower by about 30%.

We predict that passively evolving spheroids almost disappear at $K \geq 23$. The observed high- z tails of the distributions for $K \leq 23$ and for $K \leq 24$ are thus mostly due to star-forming spheroids, but the counts are likely dominated by late-type galaxies, which could account for the big peak of the estimated (from photometric redshifts) z distribution in the range $0.2 \leq z \leq 0.9$, as well as for the low- z shoulder at $K \leq 20$.

As shown by Fig. 5, according to our model, spheroids may fully account for the observed $6.7\mu\text{m}$ ISOCAM counts and for the redshift distribution derived by Sato et al. (2004; see also Flores et al. 1999). Above $\sim 100\mu\text{Jy}$ they are predicted to be mostly in the passive evolution phase, but the fraction of active star-forming spheroids increases with decreasing flux, reaching $\simeq 50\%$ at $\simeq 10\mu\text{Jy}$.

3.2 Extremely Red Objects

Extremely red objects (EROs), with $R - K > 5$, have received special attention in recent years (Daddi et al. 2000; Smith et al. 2002; Roche et al. 2002, 2003; Cimatti et al. 2002, 2003; Takata et al. 2003; Yan & Thompson 2003; Yan et al. 2004b; Webb et al. 2004; Moustakas et al. 2004), since their properties set crucial constraints on the early evolutionary phases of massive spheroidal galaxies. EROs are actually a mix of dusty star-forming and evolved galaxies formed at high redshifts (Cimatti et al. 2002, 2003; Mohan et al. 2002).

We have worked out the counts and the redshift distributions of both star-forming and passively evolving spheroidal galaxies brighter than $K = 19.2, 20, 20.3$ that, according to our model, have ERO colours (Fig. 6). This prediction is the only one, among those presented in this

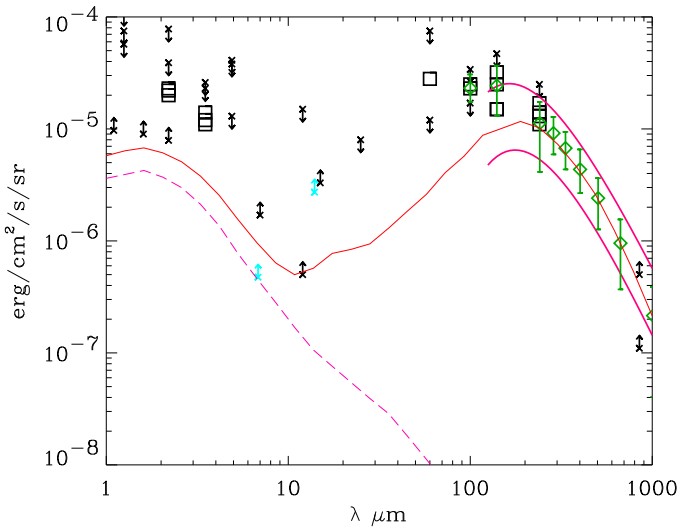


Figure 8. Contributions to the $1 - 1000\mu\text{m}$ background from passively evolving plus star-forming spheroidal galaxies (solid line). Passively evolving spheroids (dashed line) are important at $\lambda \lesssim 15\mu\text{m}$. Data are from Hauser & Dwek (2001) and Metcalfe et al. (2003).

paper, which depends strongly also on GRASIL parameters other than τ_{MC} and k (see Sect. 2.2). Indeed, the predictions at $z \gtrsim 1$ for dusty and star forming EROs require the computation of rest frame fluxes at $\lambda \lesssim 3000\text{\AA}$, which are severely dependent on details of dust obscuration.

In sharp contrast with the standard semi-analytical models, which severely under-predict this population (e.g., Somerville et al. 2004), our model somewhat over-produces the number of EROs (of both classes), in the range $1.5 \lesssim z \lesssim 2$. On the observational side, the present redshift distributions may be biased by the strong clustering of these sources and affected by sampling variance, and some may be incomplete at $z > 1$ (Yan et al. 2004b). From the theoretical point of view, it should be noted that a mild star formation activity (say at a level \sim a few % of the peak rate), either due to residual gas or induced occasionally by interactions, neglected by our simple model, could significantly decrease the predicted number of passive galaxies with ERO colours, particularly at high redshifts. To illustrate this possibility, Fig. 7 shows the effect on predicted z-distribution of EROs brighter than $K = 20$ of an ‘artificial’ (i.e. not predicted by the model equations) episode of star formation starting after the feedback from the QSO has swept out the ISM (QSO phase in the terminology of GDS04), and lasting 1 Gyr. A decline of the SFR somewhat less abrupt than implied by the GDS04 model seems also to be suggested by the results of Daddi et al. (2004), who find that star forming objects at $1.4 < z < 2$ in the K20 survey have a dust-corrected star formation somewhat higher than our prediction (Sect. 3.1). As for dusty and star forming EROs, we reminded above that our prediction depends on details of dust obscuration. For instance a shorter t_e and/or larger values of the galaxy scale length r_c would translate in less reddened objects, without affecting significantly the other results presented in this paper. An example of this is also shown in Fig. 7.

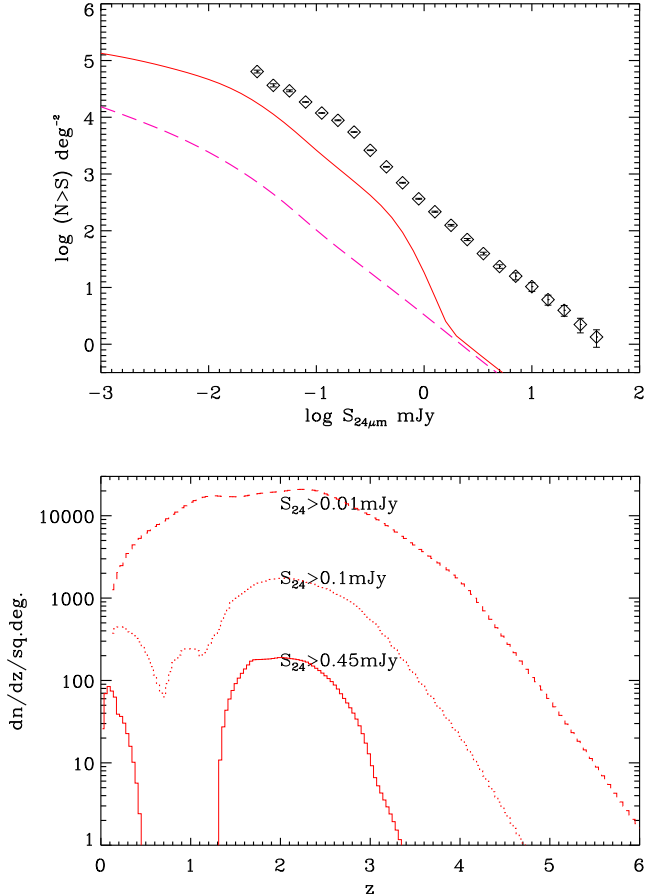


Figure 9. *Upper panel:* contributions of spheroidal galaxies to the $24\mu\text{m}$ counts predicted by our reference model compared with the Spitzer/MIPS data (Papovich et al. 2004). The long-dashed line shows the counts of passively evolving spheroids. *Lower panel:* predicted redshift distributions for $S_{24\mu\text{m}} \geq 0.45\text{ mJy}$ (the SWIRE limit, Lonsdale et al. 2003), 0.1 and 0.01 mJy.

In conclusion, it is encouraging that our model has not troubles in producing *enough* high-z objects with ERO colours. More statistic in the observations will allow us to improve the treatment of some aspects of the model, such as the amount of star formation after the QSO phase and the dust obscuration.

3.3 The IR background

A further constraint on the model comes from the IR background. In Fig. 8 we compare the $1 - 1000\mu\text{m}$ background spectrum yielded by our model with the data collected by Hauser & Dwek (2001). Longward of $\lambda \simeq 200\mu\text{m}$ star-forming spheroids alone may explain the observed background, while at shorter wavelengths, and, in particular, at the intensity peak, late-type (especially starburst) galaxies are expected to dominate.

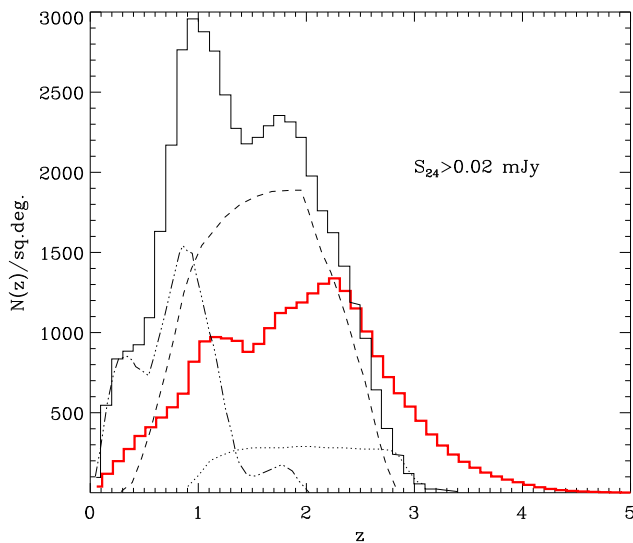


Figure 10. Redshift distribution for $S_{24\mu\text{m}} > 0.02 \text{ mJy}$. The thick histogram corresponds to our reference model for spheroids, the thin one to the model by Chary et al. (2004, their Fig. 4), which includes the contributions from low luminosity starbursts ($L_{\text{IR}} < 10^{11} L_{\odot}$, 3 dot-dashed), LIRGs with $10^{11} < L_{\text{IR}} < 10^{12} L_{\odot}$ (dashed), and ULIRGs with $L_{\text{IR}} > 10^{12} L_{\odot}$ (dotted).

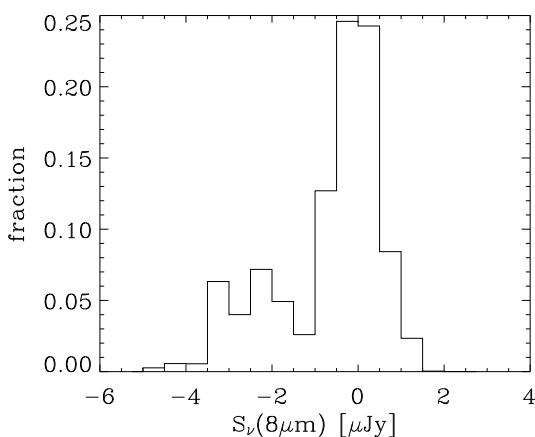


Figure 11. Expected distribution of the $8\mu\text{m}$ flux density of our model spheroids brighter than $100 \mu\text{Jy}$ at $24\mu\text{m}$ (reference model).

3.4 Contribution to $24\mu\text{m}$ Spitzer counts

Figure 9 shows the contribution from forming spheroids to the $24\mu\text{m}$ number counts, and the predicted redshift distributions at various flux limits.

In particular, our reference model predicts a non-negligible contribution, $\simeq 20\%$, to the $24\mu\text{m}$ Spitzer counts above $\simeq 0.11 \text{ mJy}$. Yan et al. (2004a) report that 13% of the detected sources do not have a counterpart at both $8\mu\text{m}$ and $0.7\mu\text{m}$, to flux limits of 20 and $0.17 \mu\text{Jy}$ respectively. In our view, this sub-population should be dominated by forming spheroids. Figure 11 reports the distribution of $S_{8\mu\text{m}}$ for our model population with $S_{24\mu\text{m}} \gtrsim 100 \mu\text{Jy}$, and shows

that only few of these sources have $S_{8\mu\text{m}} > 20 \mu\text{Jy}$. We expect that the same is true at $0.7\mu\text{m}$, although predictions at this short wavelength, probing the rest frame UV for our model sources, are very uncertain.

In Fig. 10, we have also compared the redshift distribution predicted by Chary et al. (2004, their Fig. 4) for $S_{24\mu\text{m}} > 0.02 \text{ mJy}$ with the one from our model for spheroids. Chary et al. take into account low luminosity starbursts, LIRGs and ULIRGs. Note that our model leaves room for (but does not include) populations other than forming spheroids only at redshift $\lesssim 1.5$; therefore we predict much fewer sources at high redshift as compared to Chary et al., but with a tail extending to higher z . Also according to our scenario, the populations responsible for the bulk of the 15 and $24\mu\text{m}$ counts should be at redshift $\lesssim 1.5$, since all massive halos virialized at higher z are used to build spheroids (see GDS04 for more details). The observed $24\mu\text{m}$ redshift distribution will be a strong test for our model.

3.5 Contribution to Spitzer-IRAC counts

In Fig. 12 we show the contribution of spheroidal galaxies to the Spitzer/IRAC bands, as predicted by our reference model. As expected based on results for the K and the $6.7\mu\text{m}$ bands, spheroids dominate the counts (except perhaps at the bright end), with a contribution decreasing from the near- to the mid-IR. Spheroids in the active star-forming phase dominate at faint flux density levels ($\lesssim 30 \mu\text{Jy}$).

4 DISCUSSION AND CONCLUSIONS

Granato et al. (2001, 2004a) have shown that the mutual feedback between star-forming spheroidal galaxies and the active nuclei growing in their cores can be a key ingredient towards overcoming one of the main challenges facing the hierarchical clustering scenario for galaxy formation, i.e. the fact that the densities of massive high redshift galaxies detected by SCUBA and by deep near-IR surveys are well above the predictions.

The model by GDS04 interprets the SCUBA galaxies as proto-spheroids in the process of forming most of their stars. In fact, according to this model, essentially all massive halos virializing at $z \gtrsim 1.5$ give rise to elliptical galaxies or to bulges of later type galaxies, that form at lower redshifts. The star-formation in small halos is suppressed by supernova-driven winds, so that the early star-formation occurs primarily in the more massive halos, through gigantic starbursts with star formation rates $\sim 10^3 M_{\odot}/\text{yr}$, whose duration is determined by the feedback from the active nuclei, followed by essentially passive evolution. The model can therefore be appropriately tested primarily against surveys selecting high- z galaxies, like the (sub)-mm surveys by SCUBA and MAMBO, or spheroidal galaxies, like near to mid-IR surveys.

To this end we first assessed the values of the adjustable parameter τ_{MC} of the spectrophotometric code GRASIL (Silva et al. 1998), which regulates the effect of the complex and poorly understood radiative transfer processes on the time-dependent SEDs. To properly deal with

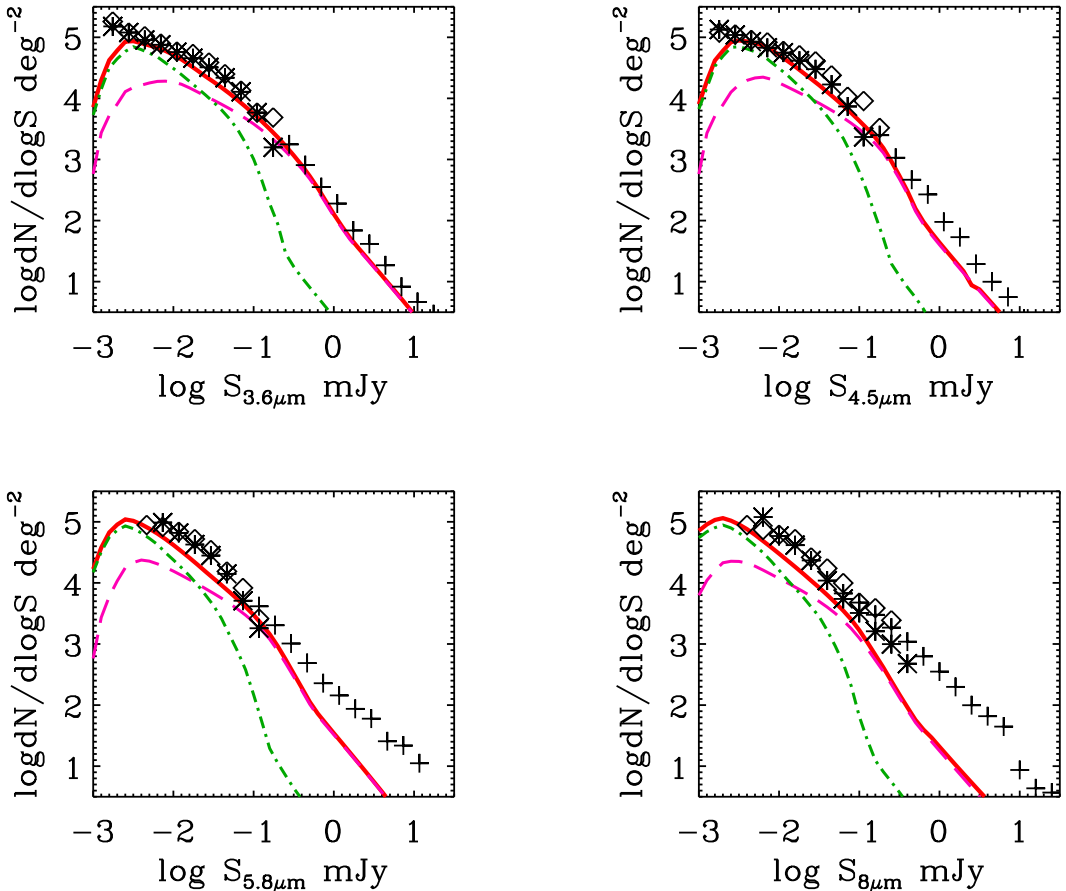


Figure 12. Contributions of spheroidal galaxies to the counts in the Spitzer/IRAC bands predicted by our reference model shown in comparison with data from Fazio et al. (2004). The thick continuous line is the total, the long dashed and dot-dashed lines are for passive and star-forming spheroids, respectively.

the extreme conditions prevailing during the intense star-formation phase of spheroidal galaxies, a new parameter, k , had to be introduced. Having fixed the values of the two parameters, and keeping the GDS04 choice for the parameters controlling the star-formation history, the chemical enrichment and the evolution of the dust and gas content of massive spheroidal galaxies, we have shown that the model accounts, on one side, for the SCUBA and MAMBO counts, corresponding to the active star-forming phase, and, on the other side, for the K -band counts for $K \lesssim 20$ –21 and for the redshift distribution of $K < 20$ galaxies, as well as for the high- z tails of redshift distributions up to $K = 24$.

Although observations unambiguously indicate that stellar populations in nearby spheroidal galaxies are old, it is possible that stars were formed in small sub-units, before the galaxy was assembled. Our results highlight a clear continuity between objects where stars formed (detected by (sub)-mm surveys) and the evolved galaxies dominating the bright K -band counts, indicating that massive spheroidal galaxies formed most of their stars when they were already assembled as single objects. As illustrated by Fig. 2, the model is remarkably successful in reproducing the observed $K < 20$ redshift distribution for $z > 1$, in contrast with

both the classical monolithic models (which overestimate the density at high- z) and the semi-analytic models (that are systematically low). For example, Somerville et al. (2004) find that their hierarchical model underproduces $K \lesssim 20.15$ ($K_{AB} \lesssim 22$ in their notation) galaxies by about a factor of 3 at $z \gtrsim 1.7$, and by an order of magnitude at $z \gtrsim 2$, while a monolithic model overproduces these galaxies by about a factor of 2 at $z \sim 2$. The GDS04 model also reproduces the bimodal distribution of colours of the Somerville et al. (2004) sample, as due to contributions of star-forming and passively evolving spheroids. The ratio of star-forming to passively evolving spheroids is also nicely consistent with the finding of Somerville et al. (2004) and Daddi et al. (2004), although the observations of the latter authors suggest a more gradual decline of the star-formation rate than implied by the current version of our model. Again, reproducing the observed colour distribution proves to be very challenging for both monolithic and standard semi-analytic models.

A specific analysis of the K -band counts and redshift distributions of EROs has been worked out, since these objects appear to provide particularly sharp constraints on galaxy evolution models. The results confirm that the GDS04 model successfully reproduces the counts, and is in

reasonably good agreement with the redshift distributions, although the need of a more sophisticated modelling of the star formation history and of dust geometry is indicated.

The mid-IR counts provided by ISOCAM, primarily at 6.7 and 15 μm , and by the Spitzer Space Telescope at several additional wavelengths and over larger areas, constrain the SEDs of spheroidal galaxies which dominate for $\lambda \lesssim 6 \mu\text{m}$, and the evolution properties (as well as the SEDs) of late-type (normal and starburst) galaxies that dominate at longer wavelengths. The ISOCAM counts at 6.7 μm and the associated redshift distribution are well fitted by the model (Fig. 5), as are the Spitzer/IRAC counts at 3.6, 4.5, and 5.8 μm .

At longer wavelengths, we expect that the contribution of starburst galaxies to the counts becomes increasingly important, particularly at bright flux densities, and to actually dominate at 24 μm (Fig. 9). Although modelling the counts of such sources is beyond the scope of the present paper, we note that, according to the GDS04 model, essentially all massive halos at $z \gtrsim 1.5$ turn into spheroidal galaxies. As a consequence, we expect a sharp drop in the redshift distribution of starburst galaxies at $z \gtrsim 1.5$, in contrast with predictions of some current phenomenological models (Dole et al. 2003; Chary & Elbaz 2001), and a high- z tail due to star-forming spheroids. For example, we expect a surface density of sources with $S_{24\mu\text{m}} > 20 \mu\text{Jy}$ and $z \simeq 2$ about 2 times lower than predicted by Chary et al. (2004, their Fig. 4).

While the scanty redshift information on 24 μm sources (Le Floc'h et al. 2004) does not allow us to test our expectations yet, such sources can be preliminarily characterized by their IR colours (Yan et al. 2004a). Remarkably, the predicted fraction of star-forming spheroids with 8 μm fluxes below the detection limit matches that found by Yan et al. (2004a). We thus interpret these sources as proto-spheroidal galaxies in the process of forming most of their stars, at typical redshifts $\simeq 2$ but with a tail extending up to $z \simeq 4$.

Moving to still longer wavelengths, we expect that star-forming spheroids start dominating the 160 μm counts below 50–100 mJy, and produce a peak at $z \sim 1.5$ in the redshift distribution, while at brighter fluxes, counts are likely dominated by low redshifts sources (Rowan-Robinson et al. 2004).

It is worth noticing that the AGN activity powered by the growing SMBHs has a small effect on the number counts of *spheroids* at all wavelengths considered here. Since the AGN SED (νL_ν) is relatively flat at optical to far-IR wavelengths and drops in the sub-mm region, the maximum AGN contribution occurs around 15 μm , at the minimum between the peak of direct starlight emission and that of dust emission (Silva, Maiolino & Granato 2004; see also Fig. 8). But, at this wavelength, the spheroids are anyway a minor component of the counts (see the upper left-hand panel of Fig. 3). The sub-mm counts are dominated by proto-spheroids with very high SFRs ($\text{SFR} \gtrsim 500 M_\odot \text{ yr}$ for sources brighter than 5 mJy), while the accretion rate onto the SMBH predicted by the model is several orders of magnitude lower (see Figs. 2 and 3 of GDS04). Therefore the AGN luminosity is generally much lower than that due to stars (it is non-negligible only for a very small fraction of the star forming phase) even allowing for a much higher mass to light conversion efficiency. On the other hand, we expect the mild AGN activity to be

detectable in X-rays in the majority of the bright SCUBA sources (Granato et al. 2004b), in keeping with the findings by Alexander et al. (2003). A detailed analysis will be presented in a forthcoming paper (Granato et al. in preparation). The counts of spheroids at $\lambda < 10 \mu\text{m}$ are dominated by objects in the passive evolution phase, for which the mass accretion rates onto the SMBHs are very low and, correspondingly, the AGN activity is very weak.

ACKNOWLEDGMENTS

Work supported in part by MIUR (through a COFIN grant) and ASI. LS and GLG acknowledge kind hospitality by INAOE where part of this work was performed, as well as support by the LSGLG foundation. Finally, we wish to thank an anonymous referee for helping us in improving the presentation of this work.

REFERENCES

Alexander D.M. et al., 2003, AJ, 125, 383
 Barger A.J., Cowie L.L., Sanders D.B., 1999, ApJL, 518, 5
 Baugh C.M., Lacey C.G., Frenk C.S., Granato G.L., Silva L., Bressan A., Benson A.J., Cole S., 2004, MNRAS, accepted (astro-ph/0406069)
 Benson A.J., Bower R.G., Frenk C.S., Lacey C.G., Baugh C.M., Cole S., 2003, ApJ, 599, 38
 Binney J., 2004, MNRAS, 347, 1093
 Blain A.W., Kneib J.-P., Ivison R.J., Smail I., 1999, ApJ, 512, 87
 Borys C., Chapman S.C., Halpern M., Scott D., 2002, MNRAS, 330, 63
 Chapman S.C., Blain A.W., Ivison R.J., Smail I.R., 2003, Nat, 422, 695
 Chapman S.C., Smail I., Ivison R.J., Helou G., Dale D.A., Lagache G., 2002, ApJ, 573, 66
 Chary R., Elbaz D., 2001, ApJ, 556, 562
 Chary R. et al., 2004, ApJS, 154, 80
 Cimatti A. et al., 2002, A&A, 381, L68
 Cimatti A. et al., 2003, A&A, 412, L1
 Cole S., Aragon-Salamanca A., Frenk C.S., Navarro J.F., Zepf S.E., 1994, MNRAS, 271, 781
 Cole S., Lacey C.G., Baugh C.M., Frenk C.S., 2000, MNRAS, 319, 168
 Conselice C.J., Bershady M.A., Dickinson M., Papovich C., 2003, AJ, 126, 1183
 Daddi E., Cimatti A., Pozzetti L., Hoekstra H., Rttgering H.J.A., Renzini A., Zamorani G., Mannucci F., 2000, A&A, 361, 535
 Daddi E. et al., 2004, ApJ, 600, L127
 Dole H. et al., 2001, A&A, 372, 702
 Dole H., Lagache G., Puget J.-L., 2003, ApJ, 585, 617
 Dole H. et al., 2004, ApJS, 154, 93
 Dwek E., 1998, ApJ, 501, 643
 Eales S., Lilly S., Webb T., Dunne L., Gear W., Clements D., Yun M., 2000, AJ, 120, 2244
 Elbaz D. et al., 1999, A&A, 351, 37
 Elbaz D., Cesarsky C.J., Chanial P., Aussel H., Franceschini A., Fadda D., Chary R.R., 2002, A&A, 384, 848
 Fazio G.G. et al., 2004, ApJS, 154, 39
 Flores H. et al., 1999, A&A, 343, 389
 Franceschini A., Aussel H., Cesarsky C.J., Elbaz D., Fadda D., 2001, A&A, 378, 1
 Franceschini A. et al., 2003, A&A, 403, 501
 Granato G.L., Lacey C.G., Silva L., Bressan A., Baugh C.M., Cole S., Frenk C.S., 2000, ApJ, 542, 710

Granato G.L., Silva L., Monaco P., Panuzzo P., Salucci P., De Zotti G., Danese L., 2001, MNRAS, 324, 757

Granato G.L., De Zotti G., Silva L., Bressan A., Danese L., 2004a, ApJ, 600, 580 (GDS04)

Granato G.L., Silva L., Danese L., De Zotti G., Bressan, A., 2004b, in Mujica R., Maiolino R., eds, Multiwavelength AGN surveys. World Scientific, Singapore, p. 379

Greve T.R., Ivison R.J., Bertoldi F., Stevens J.A., Dunlop J.S., Lutz D., Carilli C. L., 2004, MNRAS, 354, 779

Gruppioni C., Lari C., Pozzi F., Zamorani G., Franceschini A., Oliver S., Rowan-Robinson M., Serjeant S., 2002, MNRAS, 335, 831

Hammer F., Flores H., Elbaz D., Zheng X.Z., Liang Y.C., Ce-sarsky C., 2004, A&A, accepted (astro-ph/0410518)

Hauser M.G., Dwek E., 2001, ARA&A, 39, 249

Hughes D.H. et al., 1998, Nat, 394, 241

Kashikawa N. et al., 2003, AJ, 125, 53

Kauffmann G., Colberg J.M., Diaferio A., White S.D.M., 1999, MNRAS, 303, 188

Kauffmann G., White S.D.M., Guiderdoni B., 1993, MNRAS, 264, 201

Kaviani A., Haehnelt M.G., Kauffmann G., 2003, MNRAS, 340, 739

King I.R., 1972, ApJ, 174, L123

Kochanek C.S. et al., 2001, ApJ, 560, 566

Lacey C., Guiderdoni B., Rocca-Volmerange B., Silk J., 1993, ApJ, 402, 15

Lagache G., Dole H., Puget J.-L., 2003, MNRAS, 338, 555

Le Floc'h E. et al., 2004, ApJS, 154, 170

Lonsdale C.J. et al., 2003, PASP, 115, 897

Metcalfe L. et al., 2003, A&A, 407, 791

Mohan N.R., Cimatti A., Röttgering H.J.A., Andreani P., Severgnini P., Tilanus R.P.J., Carilli C.L., Stanford S.A., 2002, A&A, 383, 440

Moustakas L.A., Davis M., Graham J.R., Silk J., Peterson B.A., Yoshii Y., 1997, ApJ, 475, 445

Moustakas L.A. et al., 2004, ApJ, 600, L131

Miyazaki M. et al., 2003, PASJ, 55, 1079

Papovich C. et al., 2004, ApJS, 154, 70

Poli F. et al., 2003, ApJ, 593, L1

Pozzetti L. et al., 2003, A&A, 402, 837

Roche N.D., Almaini O., Dunlop J., Ivison R.J., Willott C.J., 2002, MNRAS, 337, 1282

Roche N.D., Dunlop J., Almaini O., 2003, MNRAS, 346, 803

Romano D., Silva L., Matteucci F., Danese L., 2002, MNRAS, 334, 444

Rowan-Robinson M. et al., 2004, MNRAS, 351, 1290

Saracco P., Giallongo E., Cristiani S., D'Odorico S., Fontana A., Iovino A., Poli F., Vanzella E., 2001, A&A, 375, 1

Sato Y. et al., 2003, A&A, 405, 833

Sato Y. et al., 2004, AJ, 127, 1285

Silva L., 1999, PhD thesis, SISSA, Trieste, Italy

Silva L., Granato G.L., Bressan A., Danese L., 1998, ApJ, 509, 103

Silva L., Maiolino R., Granato G.L. 2004, MNRAS, in press (astro-ph/0403381)

Smith G.P. et al., 2002, MNRAS, 330, 1

Somerville R.S. et al., 2004, ApJ, 600, L135

Somerville R.S., Primack J.R., 1999, MNRAS, 310, 1087

Takata T. et al., 2003, PASJ, 55, 789

Tecza M. et al., 2004, ApJ, 605, L109

Thomas D., 1999, MNRAS, 306, 655

Thomas D., Maraston C., Bender R., 2002, Ap&SS, 281, 371

Totani T., Yoshii Y., Maihara T., Iwamuro F., Motohara K., 2001, ApJ, 559, 592

Webb T., Brodwin M., Eales S., Lilly S., 2004, ApJ, 605, 645

Yan L., Thompson D., 2003, ApJ, 586, 765

Yan L. et al., 2004a, ApJS, 154, 60

Yan L., Thompson D., Soifer T., 2004b, AJ, 127, 1274